Orbital interaction and vibrational mode analyses for phase transitions of $BaTiO_3$

Tomonari Takeuchi,[a] Kazunari Yoshizawa,[b] Yoshihito Shiota,[b] Osamu Nakamura,[a] Hiroyuki Kageyama[a] and Tokio Yamabe*[b]

[a]*Osaka National Research Institute, AIST, Midorigaoka 1–8-31, Ikeda, Osaka, 563 Japan*
[b]*Department of Molecular Engineering, Kyoto University, Sakyo-Ku, Kyoto, 606–01 Japan, and Institute for Fundamental Chemistry, 34-4, Takano-Nishihiraki-cho, Sakyo-Ku, Kyoto, 606 Japan*

The phase transitions of $ATiO_3$-type perovskite structures, mainly those of barium titanate ($BaTiO_3$), are studied theoretically in terms of orbital interactions and vibrational modes. Vibrational analyses for fundamental TiO_6 clusters, up to Ti_8O_{36}, are performed with a hybrid (Hartree–Fock/density functional) method. Important structural distortions from the high symmetry cubic phase are rationalized by a second-order perturbational treatment of quantum chemistry. The orbital symmetry argument based on group theory indicates that the transition density around frontier molecular orbitals plays an important role in the motions of ions at the transition temperatures. Our orbital interaction and vibrational mode analyses of the phase transitions are consistent with the soft mode theory of Cochran.

Barium titanate ($BaTiO_3$) is a typical ferroelectric material with a relatively high relative permittivity. Because of its high relative permittivity, this compound has become one of the most important materials in the electronics industry.[1] Recently, it has been extensively studied particularly for its application as a capacitor material in dynamic random access memory (DRAM) devices.[2–4] In addition to these technological aspects, $BaTiO_3$ has also attracted much attention from the standpoint of solid-state physics and chemistry. Since this compound has a simple and very common perovskite structure and shows successive phase transitions,[5] the relationship between the crystal structure and ferroelectricity has become a major subject of research in this material.

$BaTiO_3$ is cubic above 130 °C and is paraelectric. In cubic $BaTiO_3$, Ti^{4+} is ideally located in the centre of the unit cell, surrounded by six O^{2-} ions. The Ba^{2+} ion, may be regarded as a spacer or packing ion in the three-dimensional network of TiO_6-octahedra; Ba^{2+} and O^{2-} ions together form a face-centred-cubic lattice. The cubic unit cell transforms to tetragonal below 130 °C (Curie temperature, T_C), giving rise to ferroelectricity.[6] Ti^{4+} cations in the octahedral O^{2-} cage are displaced slightly along the *c* axis, and O^{2-} ions are also displaced very slightly from their cubic positions.[7] These displacements cause a spontaneous polarization parallel to one of the original cubic [001] directions. Fig. 1(a) shows schematically the displacements of Ti^{4+} and O^{2-} ions for this phase transition.[6]

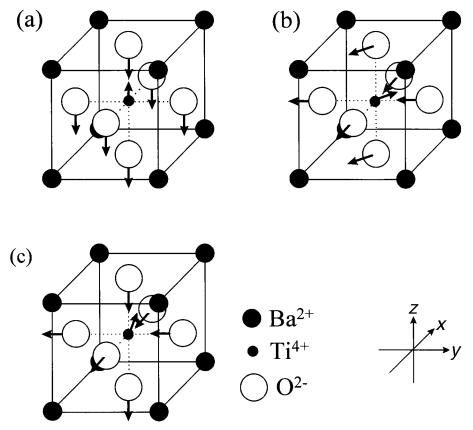

Fig. 1 Displacements of Ti^{4+} and O^{2-} ions from the original cubic to the (a) tetragonal, (b) orthorhombic, and (c) rhombohedral polymorphs.[6]

Two further phase transitions occur with decreasing temperature, to orthorhombic $\leqslant 0$ °C and to rhombohedral $\leqslant -90$ °C.[5,6] The displacement direction of the ions changes according to the symmetry of the unit cell. As shown in Fig. 1(b) and (c),[6] the Ti^{4+} ion displaces parallel to one of the original cubic [110] directions in the orthorhombic phase and to a [111] direction in the rhombohedral phase.

In addition to the bulk phase transitions described above, a dependence of the structural change on particle size at room temperature[8–10] has been reported; below a critical size of *ca.* 1 μm, the tetragonal phase becomes cubic or pseudo-cubic. Such a structural change also leads to dielectric properties which depend on grain size. The maximum permittivity was found at a size of *ca.* 1 μm.[8–10] To explain these observations, Niepce[11] proposed a core–shell model in which grains have a cubic surface and a tetragonal interior. We estimated relative amounts of the tetragonal and cubic phases in particles of 0.3–1.2 μm and analysed their grain structure from permittivity measurements on the basis of an equivalent circuit model.[12,13] By contrast, Asiaie *et al.*[14] investigated the grain structure of fine $BaTiO_3$ particles prepared hydrothermally using Raman spectroscopy, XRD and TEM, and suggested the surface layer to be tetragonal in which the long range alignment of dipole moments was destroyed by surface charge. Also Hirose and West[15] investigated ac impedance spectroscopy of $BaTiO_3$ pellets, and showed that the grain boundary is ferroelectric, similar to the grains. Although the surface structure of $BaTiO_3$ particles is still controversial, a degradation of the dielectric properties is clearly observed with decreasing particle size. The size dependence of the dielectric properties becomes more serious in thin films, but the control of the dielectric properties in fine particles and thin films is very important for further advances in electronic technology. Theoretical investigation of the phase transition of $BaTiO_3$ is therefore an important subject in ferroelectricity.

A large number of theoretical studies has been devoted to the phase transition of $BaTiO_3$.[16–21] Devonshire's phenomenological model,[18] based on thermodynamics has been widely applied to various properties of perovskite-type ferroelectrics. In the pioneering microscopic approach of Slater[19] and by Cochran,[20] Slater proposed, following Devonshire's theory, that the ferroelectric behaviour of $BaTiO_3$ arises from Lorentz correction which leads to a vanishing term in the denominator

of an expression for the relative permittivity.[19] This model assumed that the temperature dependence of the relative permittivity comes from polarization associated with displacement of Ti^{4+} ions and led to the development of soft mode theory.[16,20,21] This theory treats the lowest lattice vibrational (phonon) mode in the paraelectric phase. In cubic perovskite structures, a transverse optical (TO) mode, the 'soft phonon mode', is frozen at T_C resulting in a spontaneous polarization. Soft modes were found in $PbTiO_3$ and $SrTiO_3$ using neutron inelastic scattering[22,23] and Raman scattering[24,25] methods. However, many experimental difficulties were encountered on working with $BaTiO_3$, because the heavy and over-damped phonon disturbs the determination of the soft phonon mode.[16,17]

Soft mode theory is based on a model that $BaTiO_3$ shows a displacive phase transition at T_C. On the other hand, some researchers postulated that $BaTiO_3$ belongs to a family of order–disorder ferroelectrics. Comes *et al.*[26] proposed that $BaTiO_3$ has a some kind of disordered structure in cubic, tetragonal and orthorhombic phases, based on the observation of diffuse scattering in XRD and electron diffraction. Burns and Dacol[27] and Ito *et al.*[28] suggested the formation of microclusters above T_C, consistent with a model proposed by Comes *et al.*[26] A hyper-Raman experiment was performed recently on cubic $BaTiO_3$ by Vogt *et al.*[29] and Inoue and Akimoto.[30] The analyses and interpretations of the results were different from these two groups; Vogt *et al.* concluded that the cubic–tetragonal transition is displacive,[29] but Inoue and Akimoto regarded it as order–disorder.[30] Thus, uncertainty still remains over the nature of the cubic–tetragonal phase transition.[16,17]

In addition to the above phenomenological treatment, there have been other approaches based on solid-state electronic theory. Ikawa[31] concluded that electronic energy would stabilize the tetragonal phase at room temperature. Most solid-state physics approaches are based on interband interactions. Shukla and Sinha[32] studied the instability of vibrational modes in $BaTiO_3$ by taking account of electron–phonon coupling. They found that vibronic interactions render polar modes unstable and provided a microscopic description of the ferroelectric transition. Kristoffel and Konsin[33] also showed a vibronic interaction which causes a mixing of two close bands and leads to a phase transition. This electron–phonon interaction was applied to point defects in $BaTiO_3$ to explain the modification of ferroelectric properties upon light irradiation[34–36] and to phase-transition phenomena in other perovskite oxides.[37,38] A large-scale first principle computation of electronic states in perovskites was performed recently.[39]

In spite of the investigations mentioned above, there is still no complete understanding of the nature of the phase transitions of $BaTiO_3$ and no reliable method for predicting, for example, which phonons will be responsible for the transitions, *a priori*.[40] In the present work, we performed *ab initio* quantum chemical calculations for several clusters of TiO_6 octahedra. We ignored the Ba^{2+} ions, because a previous study[41] showed that they produce bands located far from the Fermi energy, suggesting that the electronic states of Ba^{2+} ions are less important for the phase transitions. Computational results were analysed using a transition-density analysis of Bader[42] and Pearson.[43] The orbital symmetry argument indicates that the transition density around frontier molecular orbitals, *i.e.* the highest occupied molecular orbital (HOMO) and lowest unoccupied molecular orbital (LUMO), gives useful information on the preferred motions of the constituent ions in the phase transitions.

Background to the symmetry arguments

In order to consider the behaviour of the phase transitions in $BaTiO_3$, we treat the nuclear displacements as perturbations. Using second-order perturbation theory,[42,43] we write the energy (in the ground electronic state) of distorted TiO_6 cluster configurations for extension in the ith normal coordinate, Q_i, in terms of eqn. (1),

$$E(Q_i) = E_0 + \frac{1}{2}V_{00}{}^{ii}Q_i{}^2 + \sum_k \frac{V_{0k}{}^i V_{k0}{}^i}{E_0 - E_k} \quad (1)$$

where E_0 is the energy of the undistorted cubic configuration. $V_{00}{}^{ii}$ and $V_{0k}{}^i$ are expressed by eqn. (2) and (3),

$$V_{00}{}^{ii} = \int \rho_{00} \frac{\partial^2 \phi(\boldsymbol{r}, \boldsymbol{R})}{\partial Q_i{}^2} \mathrm{d}\boldsymbol{r} \quad (2)$$

$$V_{0k}{}^i = \int \rho_{0k} \frac{\partial \phi(\boldsymbol{r})}{\partial Q_i} \mathrm{d}\boldsymbol{R} \quad (3)$$

where $\phi(\boldsymbol{r}, \boldsymbol{R})$ is the total potential of the nuclei and $\phi(\boldsymbol{r})$ is the potential interaction of the nuclei with the ith electron. The quantity ρ_{00} is the electron density for undistorted octahedral TiO_6 clusters. Thus, the second term of eqn. (1) refers to the increase in energy of the clusters when the nuclei are displaced from their original octahedral positions but the electrons are kept fixed. The third term of eqn. (1) (second-order perturbation) contains $V_{0k}{}^i$ which includes relaxation of the electron distribution through mixing between the ground state $|0\rangle$ and an exited state $|k\rangle$. The quantity ρ_{0k} appearing in $V_{0k}{}^i$ is called the transition density,[42,43] which is the electronic charge transferred within the cluster as a consequence of a certain nuclear motion. In molecular orbital terminology, ρ_{0k} is given simply by eqn. (4),

$$\rho_{0k} = c\phi_i{}^*\phi_j \quad (4)$$

where $\phi_i{}^*$ is an occupied orbital, ϕ_j is an unoccupied orbital, and c is a numerical constant. In most cases, ϕ_i and ϕ_j correspond to HOMO and LUMO, respectively, because the third term of eqn. (1) contains the energy gap expression $E_0 - E_k$ in its denominator, which means that close-lying molecular orbitals play an important role in this second-order term. The experimentally estimated energy gap of $BaTiO_3$ is 3.25 eV,[44] which is small enough to cause the second-order effect.[43]

Bader[42] interpreted the term $V_{0k}{}^i$ as the force acting on the nuclei through the relaxation of the electron distribution. This transition force is non-zero only if ρ_{0k} and Q_i have identical symmetries. Therefore the symmetry of favourable nuclear motion should be the same as the symmetry of ρ_{0k}. The following discussion of orbital interaction is based on analyses of the transition density in TiO_6 clusters.

Structures of the cubic TiO_6 clusters employed are shown in Fig. 2. For the cubic–tetragonal phase transition, we employed model clusters of (a) $TiO_6{}^{8-}$, (b) $Ti_2O_{11}{}^{14-}$, (c) $Ti_3O_{16}{}^{20-}$, and for the cubic–orthorhombic and –rhombohedral transitions, model clusters of (d) $Ti_4O_{20}{}^{24-}$ and (e) $Ti_8O_{36}{}^{40-}$, respectively. For all Ti—O atomic distances, the experimental value (2.005 Å)[6] for the cubic phase was used.

Calculations on these TiO_6 clusters were performed using the Hartree–Fock method for orbital analyses and the hybrid (Hartree–Fock/density functional) method (B3LYP)[45–47] for vibrational mode analyses. We used the minimal basis set (STO-3G) because of the size of the system considered. Our parallel calculations using the 3-21G basis set for $TiO_6{}^{8-}$ and $Ti_2O_{11}{}^{14-}$ clusters showed little difference from those calculated using STO-3G basis set, as described next. These calculations were carried out using the GAUSSIAN 94 program.[48]

Results and Discussion

Let us first look at orbital interactions in the $TiO_6{}^{8-}$ cluster. The bonding interaction between Ti 4s and O 2p orbitals is greater than that for Ti 4p–O 2p, because of radial compactness

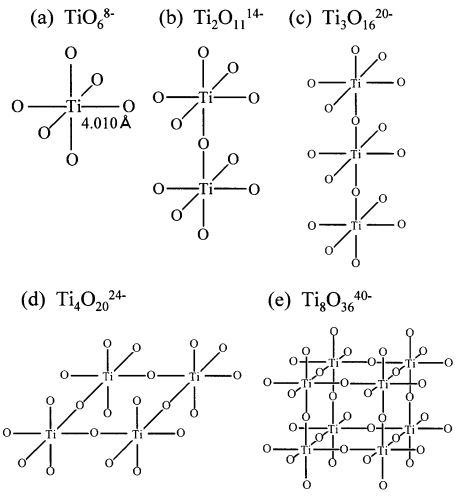

Fig. 2 Schematic representation of TiO_6 clusters employed for calculations: (a) TiO_6^{8-}, (b) $Ti_2O_{11}^{14-}$, (c) $Ti_3O_{16}^{20-}$, (d) $Ti_4O_{20}^{24-}$ and (e) $Ti_8O_{36}^{40-}$. For all first-nearest Ti—O atomic distances, the experimentally obtained value (2.005 Å)[6] for cubic phase was utilized (see text).

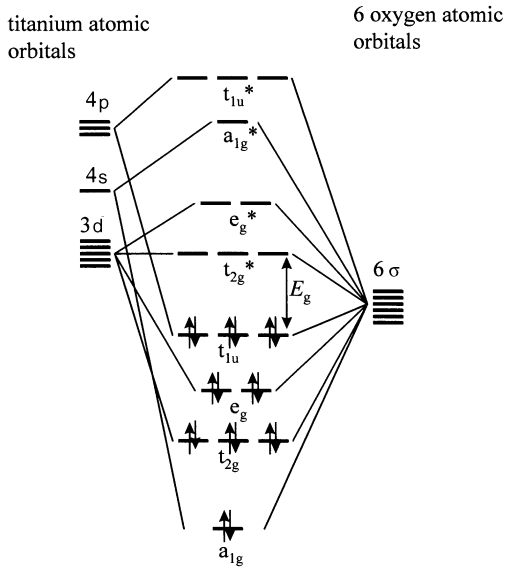

Fig. 3 Schematic molecular orbital diagram for titanium and six oxygen atoms in a TiO_6^{8-} cluster

of the Ti 4s orbital. The Ti 3d orbitals form weaker interactions with O 2p orbitals. A consequent molecular orbital diagram for a TiO_6^{8-} cluster is shown schematically in Fig. 3.

The HOMO is triply degenerate t_{1u} at 1.96 E_h (E_h = 27.212 eV) consisting of Ti and O p orbitals, whereas the LUMO is triply degenerate t_{2g} at 2.31 E_h consisting of Ti d orbitals and O p orbitals. The energy gap, E_g, between HOMO and LUMO is important for the second-order perturbation, as described above. These frontier orbitals are shown in Fig. 4.

The favourable direction of distortion is predicted from orbital symmetry and vibrational analyses.

The direct product representation of these two frontier orbitals is reduced to A_{2u}, E_u, T_{1u} and T_{2u} symmetries [eqn. (5)].

$$t_{1u} \times t_{2g} = A_{2u} + E_u + T_{1u} + T_{2u} \quad (5)$$

A_{2u} and E_u vibrations, however, do not exist, and T_{2u} distortion cannot lead to any alternative structures of $BaTiO_3$. Fig. 5 shows the calculated vibrational modes of T_{1u} with frequencies of 402 and 523 cm^{-1}.

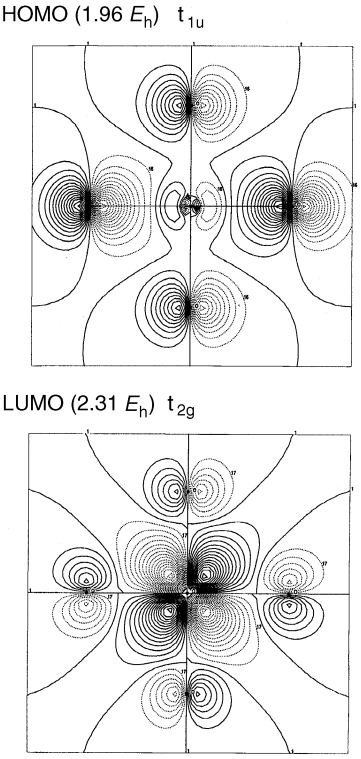

Fig. 4 Orbital patterns of the HOMO and LUMO for a TiO_6^{8-} cluster (MOLDEN[49])

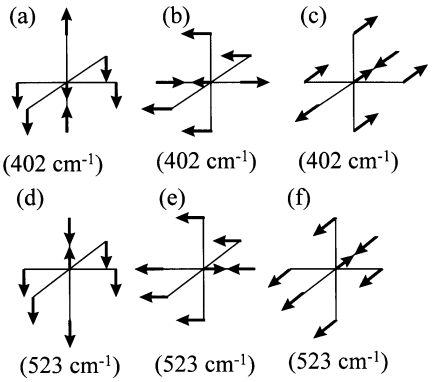

Fig. 5 Vibrational modes of T_{1u} symmetry for a TiO_6^{8-} cluster

Both modes are triply degenerate and IR active. The corresponding vibrations are observed in the IR spectrum of $BaTiO_3$; the lower-frequency Ti—O 'bending' vibration at 400 cm^{-1} corresponds to Fig. 5(a)–(c), and the higher-frequency Ti—O 'stretching' vibration at 495 cm^{-1} to Fig. 5(d)–(f).[50] The frequency values calculated on the basis of the hybrid B3LYP method are thus in good agreement with the experimental values. On the other hand, the frequencies calculated by the Hartree–Fock method were 399 and 552 cm^{-1} and therefore agreed less well with the observed values. Parallel calculations using the 3-21G basis set showed little difference from the above results; the HOMO is t_{1u} at 1.61 E_h and LUMO is t_{2g} at 2.77 E_h, with corresponding frequencies of 353 and 430 cm^{-1}. These results indicate that the STO-3G basis set is adequate in the present calculations.

As seen in Fig. 5, the T_{1u} mode of vibration draws the central Ti atom away from the centre of its octahedron. The vibration of Fig. 5(d)–(f) causes spontaneous polarization parallel to the [001] axis and leads to a tetragonal structure. Thus, the direct product of t_{1u} (HOMO) and t_{2g} (LUMO) gives the lattice distortion which leads to the tetragonal phase. This analysis indicates the applicability of the orbital symmetry argument. It signifies that the cubic–tetragonal transition is

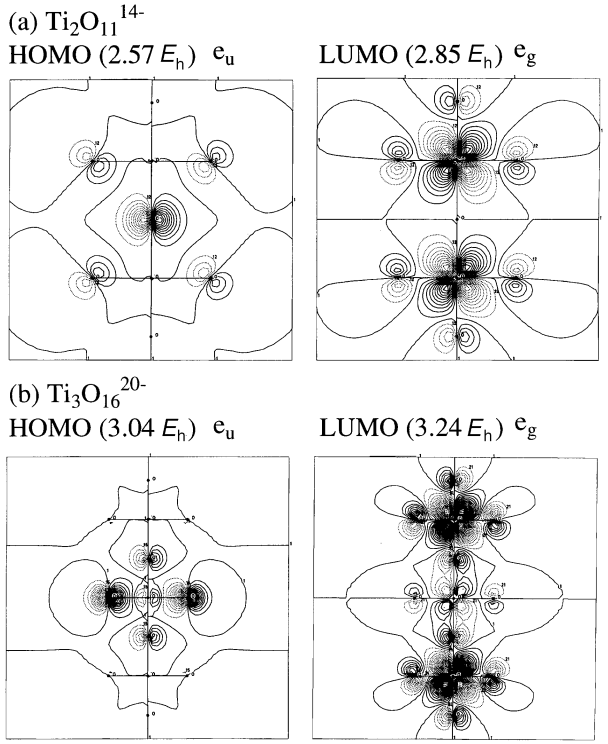

Fig. 6 Orbital patterns of the HOMO and LUMO for (a) $Ti_2O_{11}^{14-}$ and (b) $Ti_3O_{16}^{20-}$ clusters

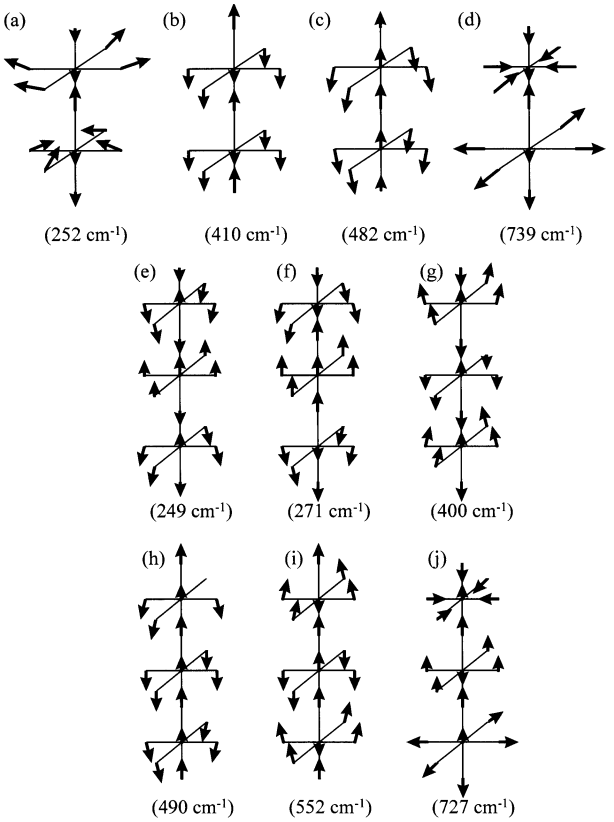

Fig. 7 Vibrational modes of A_{2u} symmetry for (a)–(d) $Ti_2O_{11}^{14-}$ and (e)–(j) $Ti_3O_{16}^{20-}$ clusters

caused by a second-order effect in perturbation theory and belongs to a second-order Jahn–Teller distortion.[43,51–53]

In soft mode theory,[16,20,21] one of the Γ_{15} modes parallel to the [001] axis, which is identical to the T_{1u} mode of Fig. 5(d), is frozen at T_C. This mode of vibration is a cause of spontaneous polarization and the ferroelectric tetragonal phase. As for the vibration which causes the cubic to tetragonal transition, the present approach is consistent with the results of soft mode theory.

We next look at the electronic states and vibrational modes of $Ti_2O_{11}^{14-}$ and $Ti_3O_{16}^{20-}$ clusters. The frontier orbitals of these clusters are shown in Fig. 6.

In both cases, the HOMO is doubly degenerate e_u, and the LUMO is doubly degenerate e_g. The orbital patterns of the HOMO and LUMO of the TiO_6^{8-} cluster appear in those of the $Ti_3O_{16}^{20-}$ cluster. The HOMO–LUMO gap becomes smaller with increasing cluster size; 0.35 E_h for TiO_6^{8-}, 0.28 E_h for $Ti_2O_{11}^{14-}$ and 0.20 E_h for $Ti_3O_{16}^{20-}$, approaching the band gap of $BaTiO_3$ (0.12 E_h).[44] This is due to the orbital interactions between the HOMO–HOMO and the LUMO–LUMO of the unit octahedron. The favourable direction of distortion is examined also from the symmetry species and the vibration analysis, as described below.

The direct product representation of e_u and e_g gives rise to A_{1u}, A_{2u}, B_{1u} and B_{2u} symmetries:

$$e_u \times e_g = A_{1u} + A_{2u} + B_{1u} + B_{2u} \quad (6)$$

A_{1u}, B_{1u} and B_{2u} vibrations, however, cannot lead to any alternative structures of $BaTiO_3$. Fig. 7 shows the calculated vibrational modes of A_{2u} for the $Ti_2O_{11}^{14-}$ and $Ti_3O_{16}^{20-}$ clusters.

These are all IR active modes. Although there is no vibration which leads to the tetragonal structure, there exist several distortions which cause a spontaneous polarization parallel to [001] axis, such as (b), (c), (e)–(i). In particular, the vibrations of (c) for $Ti_2O_{11}^{14-}$ and (h), (i) for $Ti_3O_{16}^{20-}$ show the central Ti nuclei to move away from the centre of TiO_4 plane in the opposite direction to the oxygen nuclei. This is characteristic of the distortion of Fig. 5(d), which is responsible for the cubic–tetragonal transition, as described above in TiO_6^{8-}. In addition, the calculated values [482 cm^{-1} for (c), 490 cm^{-1} for (h), and 552 cm^{-1} for (i)] are close to that of Fig. 5(d)–(f) (523 cm^{-1}) and consistent with the experimental value (495 cm^{-1}).[50] Therefore these A_{2u} vibrations seem to be effective for the distortion to the tetragonal phase. These results also support the above conclusion that the phase transition belongs to second-order Jahn–Teller distortion.

Ab initio calculations were further performed for $Ti_4O_{20}^{24-}$ and $Ti_8O_{36}^{40-}$ clusters to understand the cubic–orthorhombic and cubic–rhombohedral phase transitions. The frontier orbitals of $Ti_4O_{20}^{24-}$ are b_{1g} (HOMO) and b_{2g} (LUMO), as shown in Fig. 8(a).

The direct product representation of b_{1g} and b_{2g} is reduced to A_{2g} symmetry. Fig. 8(b) shows the calculated vibrational modes of A_{2g} for the $Ti_4O_{20}^{24-}$ cluster. As seen, A_{2g} vibrations cannot lead to any alternative structures of $BaTiO_3$. Also no distortion causes a spontaneous polarization parallel to [110] or [011], although there exist vibrations which show the central titanium nuclei moving away from the centre of TiO_6 octahedra parallel to [110] direction, accompanied by displacement of oxygen nuclei in the opposite direction. Therefore, a combination other than HOMO and LUMO in the frontier orbital region should be related to the phase transition. The MO sequence for the $Ti_4O_{20}^{24-}$ cluster is: $\cdots(a_{2u})^2(e_g)^4(b_{2u})^2(b_{1g})^2(b_{2g})^0(e_g)^0(a_{1u})^0\cdots$, although these orbitals are nearly degenerate in energy; 3.39 E_h for a_{2u}, e_g and b_{2u}, 3.41 E_h for b_{1g}, 3.64 E_h for b_{2g} and 3.66 E_h for e_g and a_{1u}. Thus, instead of HOMO and LUMO, b_{2u} (HOMO-1) and e_g (LUMO-1) could be assumed to work for transition density appearing in eqn. (3) and (4). The energy difference between these two sets of orbitals (0.27 E_h) is comparable to the HOMO–LUMO gap (0.23 E_h).

The direct product representation of b_{2u} and e_g is reduced to E_u symmetry [eqn. (7)].

$$b_{2u} \times e_g = E_u \quad (7)$$

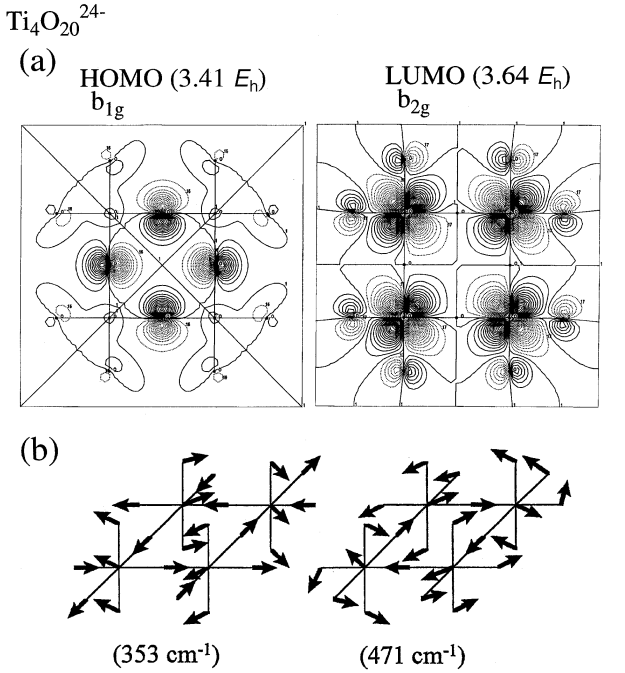

Fig. 8 (a) Orbital patterns of the HOMO and LUMO for a $Ti_4O_{20}^{24-}$ cluster; (b) vibrational modes of A_{2g} symmetry for a $Ti_4O_{20}^{24-}$ cluster

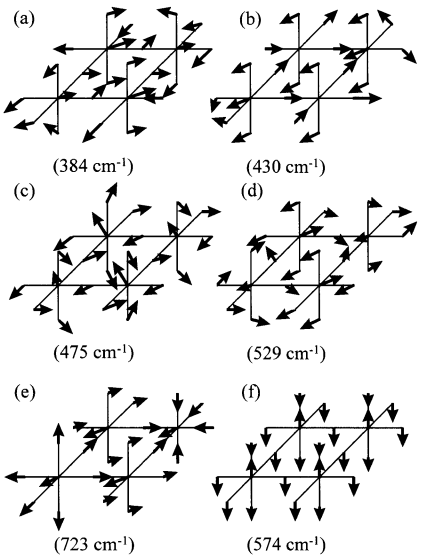

Fig. 9 (a)–(e) Vibrational modes of E_u symmetry and (f) one vibrational mode of A_{2u} symmetry for a $Ti_4O_{20}^{24-}$ cluster

The vibrational mode of E_u symmetry is IR active. Fig. 9(a)–(e) show several vibrational modes of E_u for the $Ti_4O_{20}^{24-}$ cluster.

Although no vibrational mode exactly can lead to the orthorhombic structure, the distortions in Fig. 9(a)–(e) cause a spontaneous polarization parallel to [110]. The vibrations of (c)–(e) show the central titanium nuclei moving away from the centre of TiO_6 octahedra parallel to [110] and the oxygen nuclei in the opposite direction. In other words, distortion to the orthorhombic structure appears in several TiO_6 octahedra in the $Ti_4O_{20}^{24-}$ cluster and is characteristic of the distortion which occurs in the cubic–orthorhombic transition at 0 °C. Therefore, the E_u mode of vibration would cause distortion to the orthorhombic phase.

In the $Ti_4O_{20}^{24-}$ cluster there is a particular vibration which leads to the tetragonal structure, as shown in Fig. 9(f). This vibrational mode is IR active, and its symmetry is the same as

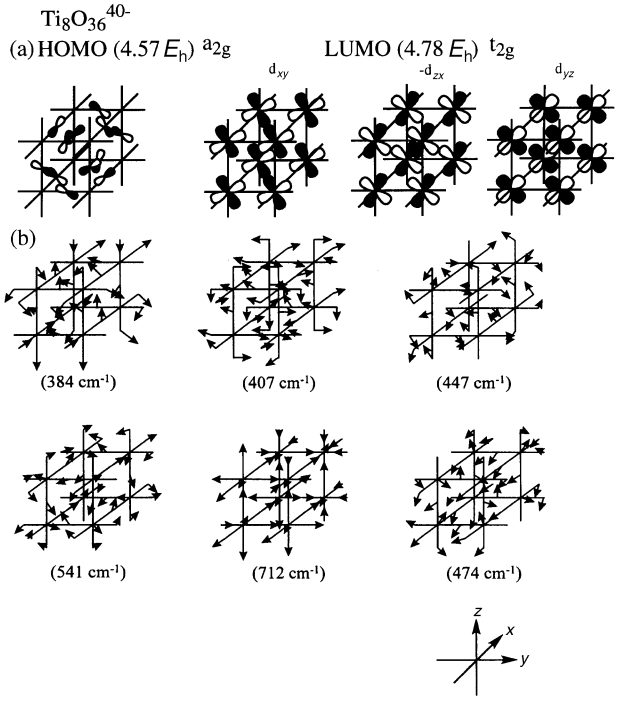

Fig. 10 (a) Orbital patterns of the HOMO and LUMO for a $Ti_8O_{36}^{40-}$ cluster; (b) vibrational modes of T_{1u} symmetry for a $Ti_8O_{36}^{40-}$ cluster

those of the $Ti_2O_{11}^{14-}$ and $Ti_3O_{16}^{20-}$ clusters, because these three clusters belong to the same point group, D_{4h}. In addition, its calculated frequency is 574 cm^{-1}, close to that of Fig. 5(d)–(f) (523 cm^{-1}). Therefore this mode is responsible for the cubic–tetragonal transition. On the basis of the present analysis, this type of vibration ought to exist in all TiO_6 based clusters. The A_{2u} symmetry is produced by the direct product of the symmetry species of the orbital combination of $a_{1g} \times a_{2u}$, $a_{1u} \times a_{2g}$, $b_{1g} \times b_{2u}$, or $b_{1u} \times b_{2g}$. These orbitals are a little far from the frontier orbital region in the $Ti_4O_{20}^{24-}$ cluster; the energy gap for these pairs is 0.07–0.12 E_h larger than the HOMO–LUMO gap. However, these gap energies are not so large as to restrict these orbitals sets to work for transition density appearing in eqn. (3) and (4). Therefore the distortion of A_{2u} symmetry is not necessarily less important than others described above.

On the basis of the present analysis, all the distortions which are responsible for the phase transitions of $BaTiO_3$ should be found in the single TiO_6^{8-} cluster. As seen in Fig. 5, vibrational modes (d)–(f) are degenerate so that a combinational mode of two of these should be also responsible for the phase transition of $BaTiO_3$. For example, a combined mode of (e) and (f) causes a spontaneous polarization parallel to [110], although it does not exactly lead to the orthorhombic structure. This is consistent with the soft mode theory,[16,20,21] in which one Γ_{15} mode parallel to [010] is frozen at about 0 °C. Since the mode parallel to [001] is frozen at about 130 °C, spontaneous polarization parallel to [011] occurs below 0 °C leading to the orthorhombic phase.

Further, we take a look at the electronic states and vibrational modes of the $Ti_8O_{36}^{40-}$ cluster in order to understand the cubic–rhombohedral transition. The frontier orbitals of $Ti_8O_{36}^{40-}$ are a_{2g} (HOMO) and t_{2g} (LUMO), as shown in Fig. 10(a).

The HOMO consists of O p orbitals, and the LUMO consists of Ti d orbitals. The direct product representation of a_{2g} and t_{2g} is reduced to T_{1g} symmetry. As for $Ti_4O_{20}^{24-}$, T_{1g} vibration in the $Ti_8O_{36}^{40-}$ cluster cannot lead to any alternative structures of $BaTiO_3$. Therefore, a combination other than HOMO and LUMO in the frontier orbital region should be related to the phase transition. The MO sequence for the

$Ti_8O_{36}^{40-}$ cluster is $\cdots(e_g)^4(t_{2u})^6(a_{2g})^2(t_{2g})^0(a_{2u})^0(e_u)^0\cdots$ although these orbitals are very close in energy; 4.56 E_h for e_g and t_{2u}, 4.57 E_h for a_{2g} and 4.78 E_h for t_{2g}, a_{2u} and e_u. So t_{2u} (HOMO−1) is implicated in eqn. (4). The direct product representation of t_{2u} and t_{2g} gives rise to A_{1u}, E_u, T_{1u}, and T_{2u} [eqn. (8)].

$$t_{2u} \times t_{2g} = A_{1u} + E_u + T_{1u} + T_{2u} \quad (8)$$

However, A_{1u}, E_u and T_{2u} modes cannot lead to any alternative structures of $BaTiO_3$. Fig. 10(b) shows several calculated vibrational modes of T_{1u} for the $Ti_8O_{36}^{40-}$ cluster. These vibrations are IR active. Note that in the vibrational mode of 712 cm^{-1} the titanium nuclei distort parallel to [111] or [111] and the oxygen nuclei distort parallel to [100] or [010]. This is characteristic of the phase transition from cubic to rhombohedral. As a consequence, this vibration causes spontaneous polarization parallel to [111]. Thus, this distortion seems to be responsible for the transition to the rhombohedral phase.

As in the discussion on the $Ti_4O_{20}^{24-}$ cluster, the distortion which leads to the rhombohedral structure should also exist in the single TiO_6^{8-} cluster. As seen in Fig. 5, a combinational mode of the degenerate three vibrations (d)–(f) should be responsible for the phase transition of $BaTiO_3$. This combined mode causes spontaneous polarization parallel to [111], although it does not exactly lead to the rhombohedral structure. This is again consistent with soft mode theory,[16,20,21] in which the last Γ_{15} mode parallel to [100] is frozen at about −90 °C. It causes spontaneous polarization parallel to [111], leading to the rhombohedral phase, since all Γ_{15} modes are frozen below −90 °C.

Let us now consider the crystal structure at the surface of fine $BaTiO_3$ particles. As described above, Niepce[11] proposed a core–shell model to explain the size-dependence of the crystal structure of $BaTiO_3$ particles.[8–10] Using our present approach, we can propose the following model as an understanding of the surface structure of fine $BaTiO_3$ particles. At the surface of fine particles, the degree of periodic order decreases. As a result, the frontier orbital levels move farther from each other, due to less interaction between the HOMO–HOMO and LUMO–LUMO of the unit octahedron. This leads to the increase in $E_0 - E_k$ appearing in eqn. (1), so that the second-order effect becomes small. Thus the appearance of the tetragonal phase might be restricted at the surface of fine particles.

We believe that our present approach based on orbital interaction analysis is applicable to other perovskite type structures. Recent extended X-ray absorption fine structure (EXAFS) for $Pb(Zn_{1/3}Nb_{2/3})O_3$ shows that Nb atoms are distorted from the octahedral positions,[54] which is the origin of the large dielectric response of this material. Also Sicron *et al.*[55] observed anti-parallel [110] displacements of Pb, Zr and O atoms for $PbZrO_3$ by the XAFS. Bugaev et al.[56] proposed Nb displacements from the centre of NbO_6 octahedron in $LiNbO_3$, $NaNbO_3$ and $KNbO_3$ from EXAFS analysis. All these observations would be rationalized by our orbital interaction and vibrational mode analyses.

Conclusions

We have examined from a quantum chemical viewpoint the phase transition of $ATiO_3$ structure, mainly concerning $BaTiO_3$. The second-order term in the perturbational treatment of Bader and Pearson plays an important role in nuclear distortion at the phase transitions. The preferred distortions which arise from the orbital interaction were predicted using an analysis of the transition density near the frontier orbital region. Our orbital interaction and vibrational mode analyses of the phase transitions are consistent with the soft mode theory of Cochran. We believe that our approach will be useful for the comprehensive understanding of the role of orbital interactions in the phase transitions of perovskite type structures.

We wish to express our gratitude to Professor Anthony Roy West of the University of Aberdeen for stimulating discussion. Thanks are due to a Grant-in-Aid for Scientific Research from the Ministry of Education, Science and Culture of Japan and the Japan Society for the Promotion of Science (JSPS-RFTF96 P00206).

References

1 J. Nowotny and M. Rekas, *Key Eng. Mater.*, 1992, **66** & **67**, 45.
2 R. Bacsa, P. Ravindranathan and J. P. Dougherty, *J. Mater. Res.*, 1992, **7**, 423.
3 E. Shi, C. R. Cho, M. S. Jang, S. Y. Jeong and H. J. Kim, *J. Mater. Res.*, 1994, **9**, 2914.
4 A. T. Chien, J. S. Speck, F. F. Lange, A. C. Daykin and C. G. Levi, *J. Mater. Res.*, 1995, **10**, 1784.
5 J. Nowotny, *Electronic Ceramic Materials*, Trans Tech, Brookfield, VT, 1992.
6 H. F. Kay and P. Vousden, *Philos. Mag.*, 1949, **40**, 1019.
7 L. L. Hench and J. K. West, *Principles of Electronic Ceramics*, John Wiley & Son, New York, 1990.
8 G. Arlt, D. Hennings and G. de With, *J. Appl. Phys.*, 1985, **58**, 1619.
9 D. Hennings, *Int. J. High Technol. Ceram.*, 1987, **3**, 91.
10 K. Uchino, E. Sadanaga and T. Hirose, *J. Am. Ceram. Soc.*, 1989, **72**, 1555.
11 J. C. Niepce, in *Surface and Interface of Ceramic Materials*, ed. L. C. Dufour, C. Monty and G. Petot-Ervas, Kluwer, Dordrecht, Germany, 1989, p. 521.
12 T. Takeuchi, K. Ado, T. Asai, H. Kageyama, Y. Saito, C. Masquelier and O. Nakamura, *J. Am. Ceram. Soc.*, 1994, **77**, 1665.
13 T. Takeuchi, K. Ado, H. Kageyama, K. Honjo, Y. Saito, C. Masquelier and O. Nakamura, *J. Ceram. Soc. Jpn.*, 1994, **102**, 1177.
14 R. Asiaie, W. Zhu, S. A. Akbar and P. K. Dutta, *Chem. Mater.*, 1996, **8**, 226.
15 N. Hirose and A. R. West, *J. Am. Ceram. Soc.*, 1996, **79**, 1633.
16 T. Nakamura, *Kyouyudentai to kouzou souteni* (*Ferroelectric Materials and Their Phase Transitions*), Shoukabo, Tokyo, 1992.
17 N. Hirose, Ph. D. Thesis, *Impedance Characterization of Conducting Materials*, University of Aberdeen, UK, 1995, ch. 6.
18 A. F. Devonshire, *Philos. Mag.*, 1949, **40**, 1040.
19 J. C. Slater, *Phys. Rev.*, 1950, **78**, 748.
20 W. Cochran, *Phys. Rev. Lett.*, 1959, **3**, 412.
21 H. Takahasi, *J. Phys. Soc. Jpn.*, 1961, **16**, 1685.
22 G. Shirane, J. D. Axe, J. Harada and J. P. Remeika, *Phys. Rev. B*, 1970, **2**, 155.
23 R. A. Cowley, *Phys. Rev. A*, 1964, **134**, 981.
24 G. Burns and B. A. Scott, *Phys. Rev. B*, 1973, **7**, 3088.
25 P. A. Fleury and J. M. Worlock, *Phys. Rev.*, 1968, **174**, 613.
26 R. Comes, M. Lambert and A. Guinier, *Solid State Commun.*, 1968, **6**, 715.
27 G. Burns and F. H. Dacol, *Solid State Commun.*, 1982, **42**, 9.
28 K. Ito, L. Z. Zeng, E. Nakamura and N. Mishima, *Ferroelectrics*, 1985, **63**, 29.
29 H. Vogt, J. A. Sanjurjo and G. Rossbroich, *Phys. Rev. B*, 1982, **26**, 5904.
30 K. Inoue and S. Akimoto, *Solid State Commun.*, 1983, **46**, 441.
31 H. Ikawa, in *Ceramic Transactions, Dielectric Ceramics: Processing, Properties, and Applications*, ed. K. M. Nair, J. P. Guha and A. Okamoto, American Ceramic Society, Westerville, OH, 1993, vol. 32, p. 19.
32 G. C. Shukla and K. P. Sinha, *J. Phys. Chem. Solids*, 1966, **27**, 1837.
33 N. Kristoffel and P. Konsin, *Phys. Status. Solidi*, 1967, **21**, K39.
34 G. Chanussot and C. Thiebaud, *Ferroelectrics*, 1974, **8**, 665.
35 G. Chanussot, *Ferroelectrics*, 1974, **8**, 671.
36 G. Chanussot, *Ferroelectrics*, 1976, **13**, 313.
37 C. Totsuji and T. Matsubara, *J. Phys. Soc. Jpn.*, 1991, **60**, 3549.
38 C. Totsuji and T. Matsubara, *Seramikkusu*, 1992, **27**, 693.
39 W. Zhong, D. Vanderbilt and K. M. Rabe, *Phys. Rev. Lett.*, 1994, **73**, 1861.
40 R. D. King-Smith and D. Vanderbilt, *Phys. Rev. B,* 1994, **49**, 5828.
41 T. Wolfram, *Phys. Rev. B*, 1973, **7**, 1677.
42 R. F. W. Bader, *Can. J. Chem.*, 1962, **40**, 1164.
43 R. G. Pearson, *J. Am. Chem. Soc.*, 1969, **91**, 4947.
44 W. S. Baer, *J. Phys. Chem. Solids*, 1967, **28**, 677.

45 C. Lee, W. Yang and R. G. Parr, *Phys. Rev. B*, 1988, **37**, 785.
46 B. Miehlich, A. Savin, H. Stoll and H. Preuss, *Chem. Phys. Lett*., 1989, **157**, 200.
47 A. D. Becke, *J. Chem. Phys*., 1993, **98**, 5648.
48 M. J. Frisch, G. W. Trucks, H. B. Schlegel, P. M. W. Gill, B. G. Johnson, M. A. Robb, J. R. Cheeseman, T. Keith, G. A. Petersson, J. A. Montgomery, K. Raghavachari, M. A. Al-Laham, V. G. Zakrzewski, J. V. Ortiz, J. B. Foresman, C. Y. Peng, P. Y. Ayala, W. Chen, M. W. Wong, J. L. Andres, E. S. Replogle, R. Gomperts, R. L. Martin, D. J. Fox, J. S. Binkley, D. J. Defrees, J. Baker, J. P. Stewart, M. Head-Gordon, C. Gonzalez and J. A. Pople, GAUSSIAN 94, Gaussian Inc., Pittsburgh, Pennsylvania, 1995.
49 G. Schaftenaar, MOLDEN, CAOS/CAMM Center Nijmegen, Toernooived, Nijmegen, Netherlands, 1991.
50 J. T. Last, *Phys. Rev*., 1957, **105**, 1740.
51 J. K. Burdett, *Chemical Bonding in Solids*, Oxford University Press, New York, 1995.
52 M. Gerloch, *Inorg. Chem*., 1981, **20**, 638.
53 J. K. Burdett, *Inorg. Chem*., 1981, **20**, 1959.
54 P. Li, Y. Wang and I-W. Chen, *Ferroelectrics*, 1994, **158**, 235.
55 N. Sicron, Y. Yacoby and E. A. Stern, in *International Conference on X-ray Absorption Fine Structures IX*, Grenoble, France, August 1996.
56 L. Bugaev, V. Shuvaeva, I. Alekseenko, Z. Zhuchkov and E. Husson, in *International Conference on X-ray Absorption Fine Structures IX*, Grenoble, France, August 1996.

Paper 6/07475H; *Received* 4*th November*, 1996